A metasurface optical modulator using voltage-controlled population of quantum well states

Raktim Sarma, Salvatore Campione, Michael Goldflam, Joshua Shank, Jinhyun Noh, Loan T. Le, Michael D. Lange, Peide D. Ye, Joel Wendt, Isaac Ruiz, Stephen W. Howell, Michael Sinclair, Michael C. Wanke, and Igal Brener

Citation: Appl. Phys. Lett. **113**, 201101 (2018); doi: 10.1063/1.5055013

View online: https://doi.org/10.1063/1.5055013

View Table of Contents: http://aip.scitation.org/toc/apl/113/20

Published by the American Institute of Physics

Articles you may be interested in

Multipolar-interference-assisted terahertz waveplates via all-dielectric metamaterials
Applied Physics Letters **113**, 201103 (2018); 10.1063/1.5063603

A high numerical aperture, polarization-insensitive metalens for long-wavelength infrared imaging
Applied Physics Letters **113**, 201104 (2018); 10.1063/1.5050562

Phase control of plasmon enhanced two-photon photoluminescence in resonant gold nanoantennas
Applied Physics Letters **113**, 211101 (2018); 10.1063/1.5051381

Characterization of longitudinal acoustic phonons in InGaAsP multiple quantum wells by asynchronous optical sampling
Applied Physics Letters **113**, 201102 (2018); 10.1063/1.5041475

Broadband visible-to-telecom wavelength germanium quantum dot photodetectors
Applied Physics Letters **113**, 181101 (2018); 10.1063/1.5052252

Controllable generation of second-harmonic vortex beams through nonlinear supercell grating
Applied Physics Letters **113**, 221101 (2018); 10.1063/1.5050423

A metasurface optical modulator using voltage-controlled population of quantum well states

Raktim Sarma,[1,a)] Salvatore Campione,[1] Michael Goldflam,[1] Joshua Shank,[1] Jinhyun Noh,[2] Loan T. Le,[3] Michael D. Lange,[3] Peide D. Ye,[2] Joel Wendt,[1] Isaac Ruiz,[1] Stephen W. Howell,[1] Michael Sinclair,[1] Michael C. Wanke,[1] and Igal Brener[1,4,a)]
[1]Sandia National Laboratories, Albuquerque, New Mexico 87185, USA
[2]School of Electrical and Computer Engineering and Birck Nanotechnology Center, Purdue University, West Lafayette, Indiana 47907, USA
[3]Northrop Grumman Corporation, Redondo Beach, California 90278, USA
[4]Center for Integrated Nanotechnologies, Sandia National Laboratories, Albuquerque, New Mexico 87185, USA

(Received 5 September 2018; accepted 28 October 2018; published online 13 November 2018)

The ability to control the light-matter interaction with an external stimulus is a very active area of research since it creates exciting new opportunities for designing optoelectronic devices. Recently, plasmonic metasurfaces have proven to be suitable candidates for achieving a strong light-matter interaction with various types of optical transitions, including intersubband transitions (ISTs) in semiconductor quantum wells (QWs). For voltage modulation of the light-matter interaction, plasmonic metasurfaces coupled to ISTs offer unique advantages since the parameters determining the strength of the interaction can be independently engineered. In this work, we report a proof-of-concept demonstration of a new approach to voltage-tune the coupling between ISTs in QWs and a plasmonic metasurface. In contrast to previous approaches, the IST strength is here modified via control of the electron populations in QWs located in the near field of the metasurface. By turning on and off the ISTs in the semiconductor QWs, we observe a modulation of the optical response of the IST coupled metasurface due to modulation of the coupled light-matter states. Because of the electrostatic design, our device exhibits an extremely low leakage current of ~6 pA at a maximum operating bias of +1 V and therefore very low power dissipation. Our approach provides a new direction for designing voltage-tunable metasurface-based optical modulators. *Published by AIP Publishing.* https://doi.org/10.1063/1.5055013

The study and control of light-matter interactions are not only important from a fundamental scientific point of view but also because they can lead to new optoelectronic device concepts. Different regimes of the light-matter interaction can be obtained when a fundamental material excitation with an optical transition is coupled to some form of optical cavity. Particularly, the regime of strong coupling can lead to significant modifications of transmission and reflection spectra. This is typically evidenced by a spectral splitting of the resonance feature of the material excitation into two polariton branches separated by the Rabi splitting. The ability to vary this matter-cavity coupling with some external stimuli has been an active area of research for decades.

Recently, plasmonic metasurfaces have provided new ways to interact strongly with various types of material excitations such as electronic transitions in dye molecules,[1,2] cyclotron resonances,[3] phonons,[4] epsilon-near-zero modes,[5,6] and intersubband transitions (ISTs) in quantum wells (QWs).[7–9] The last offers some peculiar advantages for controlling the interaction strength with an applied bias, important for practical optoelectronic devices. In a coupled IST/metasurface system, the parameters that determine the coupling strength can be independently engineered. For example, the resonant frequency and the near field distribution can be engineered by adjusting the shape and size of the resonators forming the metasurface. The frequency and oscillator strength of the optical transition realized by the IST in QWs can be chosen by appropriate heterostructure design and QW doping density. In addition, the spatial overlap between the plasmonic mode and the ISTs can be controlled via the thickness of the QW stack.

Along with fundamental studies, metasurface-IST coupled hybrid systems have been studied for various applications such as ultrathin nonlinear metasurfaces,[10–13] IST-based light emitting diodes,[14] voltage-tunable filters,[8] and optical modulators.[9] In the context of practical tunable filters and modulators, it is essential to modulate the coupling between the two resonant systems using a bias voltage. While various voltage-tunable approaches to realize metasurface based modulators and filters have been reported such as using conducting-oxides such as ITO,[6,15–17] graphene,[18–22] and epsilon-near-zero modes in highly doped semiconductors,[5,23] a coupled IST/metasurface system offers a significant advantage of having the flexibility of wide tunability of the operational wavelength of the device. Since the operational wavelength in a metasurface/IST coupled device is determined by the IST transition frequency, the latter can be tuned by (i) the heterostructure materials and (ii) adjusting the thickness of the QWs, where the spectral tuning of the IST is limited by the conduction band offset of the

[a)]Authors to whom correspondence should be addressed: rsarma@sandia.gov and ibrener@sandia.gov

semiconductor heterostructure being used. For example, in an $In_{0.53}Ga_{0.47}As/Al_{0.48}In_{0.52}As$ multi-QW heterostructure, the conduction band offset is $\sim$0.53 eV. The IST transitions using such a heterostructure can therefore be scaled to span most of the mid-IR wavelength range including the atmospheric transmission window of 8–12 μm which is extremely important for applications ranging from spectroscopy, material processing, thermal imaging, chemical and biomolecular sensing, and defense. On the other hand, existing approaches using conductive oxides such as ITO work mostly in the near IR and cannot be scaled to such long wavelengths. Graphene-based approaches show limited tunability but require high operation voltages and complex device architectures.[21] Finally, the approach of field effect modulation of the carrier density using epsilon-near-zero modes in highly doped III-V semiconductors works well at long-IR wavelengths but it is difficult to scale to much shorter wavelengths due to the decreasing depletion width for the higher doping densities required to operate in the near IR.

Prior work of voltage-controlled spectral or intensity modulation using IST-metasurface coupled devices has relied on the quantum-confined Stark effect[8,9] to change the IST resonant frequency. Although the Stark effect leads to a significant spectral or amplitude modulation of reflectivity and/or transmission, it also requires a relatively large current flow on the order of mA.[8,9] The current enables the homogenization of the large electric field across many heavily doped quantum wells needed for the Stark effect. Without the current flow, the charge in the heavily doped QW nearest to the electrical contacts screens the electric field from the other adjacent QWs, leading to no measurable quantum confined Stark effect for most of the QWs in the sample. Finally, attempting to deplete carriers from several highly doped QWs is also impractical due to the same screening argument and due to the thin depletion width obtained for doping densities higher than 10^{18} cm^{-3}.

In this paper, we present a proof-of-concept experimental demonstration of a new approach to tune the optical response of a plasmonic metasurface using a voltage bias to control its coupling to ISTs. Instead of tuning the resonance frequency of the IST through Stark tuning, we tune the IST strength by changing the QW electron population via an applied voltage bias, leading to transfer of electrons from an electron reservoir to the wells. In contrast to the Stark shift approach, our approach does not require a continuous flow of current, thus reducing ohmic losses and power consumption. When no bias is applied, there is an absence of electrons in our undoped QWs, and therefore, the ISTs are turned off—the metasurface and IST are uncoupled and only the spectral response of the metasurface is present. When a bias is applied, electrons are electrostatically pulled from the electron reservoir and accumulate in the QWs. The enhancement of electron density in the QWs turns the ISTs on and leads to coupling between the metasurface and the ISTs. This, in turn, leads to modulation of the optical response (reflectivity or transmission) of the metasurface. To enable the electrons to quickly move in and out of the QWs, the QWs are designed so that their ground states would align at a certain bias to enhance the tunneling rate between the wells and reservoir. As a final refinement, we used a high-κ dielectric barrier rather than a semiconductor barrier to prevent leakage current when the device is biased. While field-induced electron transfer has been used to frequency tune the spectral response of QW infrared photodetectors,[24,25] it has not been used to modulate the optical response of a metasurface-IST coupled system. Field-induced accumulation therefore offers a new low-dissipation approach to modulate the optical response of a metasurface coupled to ISTs using a bias voltage.

To construct our devices, we fabricated a metallic 2D plasmonic metasurface on a high-κ dielectric deposited on top of a semiconductor heterostructure (grown by molecular-beam epitaxy) as shown schematically in Figs. 1(a) and 1(d); the heterostructure is shown in Fig. 1(b). Although there are technically 7 quantum wells, we consider the structure to consist of three effective $In_{0.53}Ga_{0.47}As$ QWs and one InP QW all separated with $Al_{0.48}In_{0.52}As$ barriers [Fig. 1(b)]. The QWs and barriers are undoped and are grown above a 90 nm $In_{0.53}Ga_{0.47}As$ layer with average doping density of $N_D = 2 \times 10^{18}$ cm^{-3}, which acts as an electron reservoir and bottom contact simultaneously. The entire epitaxial stack is grown on a semi-insulating InP substrate. The QW thicknesses are chosen such that the IST transition between the ground state and the first excited state in each well is at a wavelength of $\sim$11 μm. The InP layer in each of the $In_{0.53}Ga_{0.47}As$ QWs allows the IST in all the wells to have the same wavelength while keeping the ground state levels simultaneously aligned at a specific bias. Figure 1(a) shows schematically the electron density distribution of the device

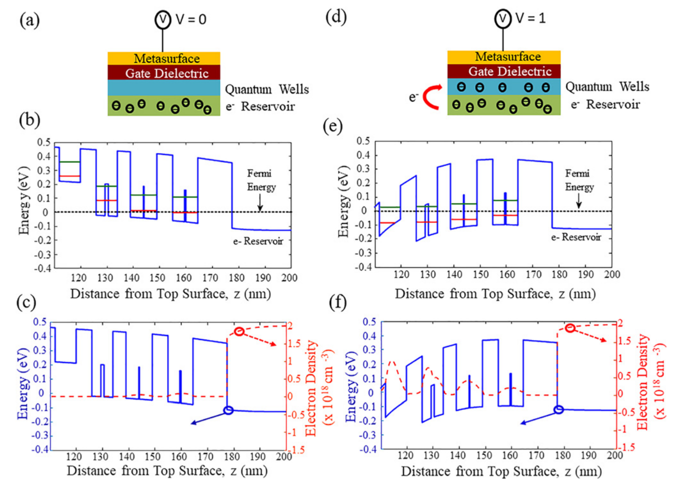

FIG. 1. (a) Schematic showing the cross-section of the device and the corresponding electron densities at zero bias, for which almost all electrons are in the electron reservoir, and the QWs have negligible electrons. (b) Self-consistent band structure calculation for the multi-QW structure using a Schrodinger-Poisson solver at zero bias (blue). The thickness of the first InP QW is 8 nm and those of the InGaAs QWs (in the order of increasing z) are 6.75/9.75/9 nm. The thicknesses of the InP layer in the InGaAs QWs are 1.25/0.25/0.5 nm, respectively. The eigenvalues for the ground (red) and first excited states (green) of all the QWs are shown. The wavelength corresponding to the ground to 1st excited state transition is 11 μm. The black dotted line signifies the Fermi energy showing that only the ground state of the first QW near the electron reservoir is occupied. (c) Plot of the band structure (left y axis) and corresponding electron density (right y axis) for zero bias. Only the first QW has some electrons. (d) Schematic showing the electron densities at V = 1V. On applying a bias, some of the electrons get electrostatically pulled from the reservoir, and they populate the QWs. (e) Self-consistent band structure calculation for the multi-QW structure at a bias of 1 V. The electronic energies get lowered, and the energy levels of the ground states and first excited states of all the QWs become energetically aligned. The ground states of all the QWs are now below the Fermi energy. (f) Plot of the band structure (left y axis) and the corresponding electron density (right y axis) for bias V = 1 V. All the QWs ground states are now populated by electrons.

for a bias of 0 V. The corresponding self-consistent Schrodinger-Poisson conduction band structure calculation of the multi-QW structure is shown in Fig. 1(b); at a bias of 0 V, only the ground state of the QW closest to the electron reservoir is below the Fermi energy and is therefore occupied. Figure 1(c) shows the corresponding spatial distribution of the electron density in the heterostructure. Since the QWs have negligible electron density, the ISTs in the QWs are inactive. Upon the application of a positive bias to the metasurface, the ground state energies of the QWs drop below the Fermi energy in the reservoir (without changing the energy difference between the ground and the first excited state), and at a certain voltage, the energy levels of all the QWs become aligned. The alignment of the ground states enhances tunneling from the electron reservoir and leads to filling of the ground states of all the QWs simultaneously.[26] Figure 1(d) shows schematically the new electron density distribution of the device for a bias of 1 V, and the corresponding band structure calculation is shown in Fig. 1(e), where at 1 V, the ground states of all the QWs are nearly aligned and are below the Fermi energy. Figure 1(f) shows the corresponding spatial distribution of the electron density for the different QWs. The ground states in each well are now populated, and the ISTs are effectively "turned on." The final carrier concentration in the wells depends on the electron concentration of the reservoir and the heterostructure design. In this study, we chose the doping density such that the doped $In_{0.53}Ga_{0.47}As$ reservoir layer has a plasma wavelength which is much longer than the IST wavelength. This ensures that the modulation of the metasurface response we observe experimentally is due to voltage-induced coupling between the metasurface and the IST and not from an epsilon-near-zero mode[5] supported by the doped layer.

The fabricated metasurface in Fig. 2(a) consists of a plane of metal with a periodic array of inverse "dogbone" resonators (H shaped holes). This configuration was chosen because all the metal is electrically connected and can be used as a metallic gate for voltage biasing. Furthermore, the "dogbone" resonator [Fig. 2(b)] shape was selected for its high capacitance, which enhances coupling between the metasurface resonances and the ISTs.[27] The dimensions of the unit cell of this periodic array, shown in Fig. 2(b), were chosen so that the dipole resonances of the metasurface had the same resonant wavelength as the IST wavelength which leads to coupling between the two resonances. The evanescent field of the dipole resonances of the metasurface generates electric field components normal to the surface, which enables the electric field to couple to the ISTs.[7–9] At 0 V (*IST OFF* state), the QW electron concentration is negligible, and the wells behave as dielectric layers. In this case, the optical response of the device is given by the uncoupled metasurface optical response. At 1 V (*IST ON* state), the QWs are populated, and the near fields of the metasurface drive the ISTs. This leads to coupling between the two resonant systems and a modified optical response. We note here that the decay lengths of evanescent fields of the dipole resonances are typically on the order of a few hundred nanometers.[11,28] Since the heterostructure used for this study has only 4 QWs (spanning only ~60 nm), we therefore do not obtain complete

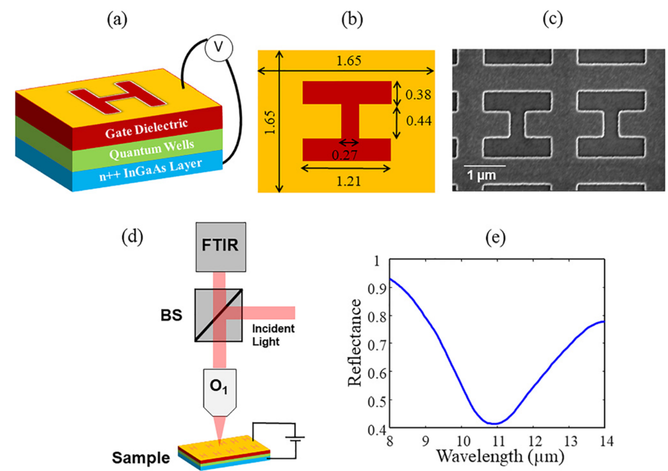

FIG. 2. (a) Three-dimensional unit cell schematic of the metasurface-semiconductor hybrid structure. (b) Dimensions of the dogbone complementary resonator (scale factor 1.0) in micrometers. When the scaling factor is varied, all marked dimensions are scaled accordingly. (c) Scanning electron micrograph of a fabricated metasurface with resonators of scale factor 1.0. The "dogbone" shapes are openings in an otherwise continuous metal film. (d) Schematic of the experimental setup used to measure the voltage-induced modulation of reflectance from the metasurface. The source light is rerouted using a beam splitter (BS) and then focused onto the sample using an objective (O_1) with NA of 0.4. The reflected light is collected using the same objective and is rerouted to an FTIR spectrometer. (e) Room temperature FTIR reflectance measurements of a metasurface with resonators of scale factor 1.35. The resonance is centered around the IST wavelength of 11 μm.

spatial overlap of the active region consisting of the QWs with the plasmonic mode.

A 10 nm HfO_2 layer deposited using Atomic Layer Deposition (ALD) separates the metallic gate and the multi-QW structures and acts as the high-κ gate dielectric. To ensure a high-quality interface between the gate dielectric and the semiconductor heterostructure, we added a 1 nm interlayer of Al_2O_3.[29] Figure 2(c) shows a scanning electron micrograph of a metasurface fabricated using electron-beam lithography to pattern the "dogbones." It was followed by evaporation to deposit Ti/Au (5 nm/100 nm), and then, the metal was lifted-off to complete the process. To access the highly doped layer and to define the area of a device, wet-chemical etching was used to etch away the gate dielectric and the QWs around $150 \times 250\,\mu$m mesas. Electrical contact to the highly doped layer was made by depositing a Ti/Au/Ag/Au ohmic contact on top of the etch-exposed highly doped $In_{0.53}Ga_{0.47}As$ layer. The bare resonance frequency of the metasurface scales with the dimensions of the metasurface unit cell. Therefore, to ensure that we obtained a device such that the metasurface resonance frequency was resonant

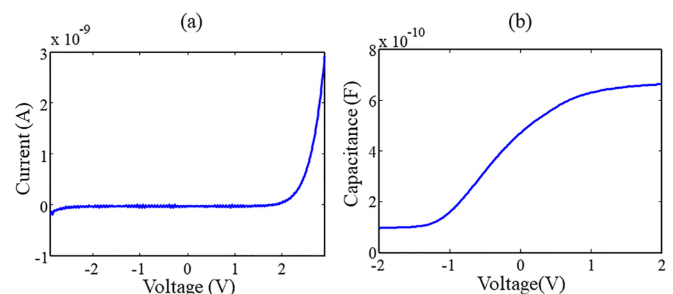

FIG. 3. (a) Static current-voltage characteristics of the device. (b) Capacitance-voltage measurements at the frequency of 1 kHz.

with the IST frequency, we fabricated resonators with different geometric scaling factors on top of the same heterostructure. Figure 2(d) shows a schematic of the experimental setup used to measure the reflectance from the fabricated metasurface. Figure 2(e) shows room temperature reflectance spectra (without any bias) of a metasurface with the resonators scaled 1.35× larger than the dimensions in Fig. 2(b). The spectra were obtained using a Fourier Transform Infrared (FTIR) spectrometer with a microscope objective of NA = 0.4. The raw metasurface reflectance spectra were referenced against the reflectance spectra of an unpatterned gold surface to remove the spectral dependency of the FTIR spectrometer and extract the metasurface response. As shown in Fig. 2(e), a scale factor of 1.35 places the metasurface resonance near the desired wavelength of 11 μm. This scale factor was used in the voltage-tuning experiment and simulations.

Figure 3(a) shows the device current as a function of applied bias. As described above, our design requires a bias of +1 V for the electronic bands to align and to inject electrons into all the QWs. For voltages between ±1 V, leakage currents are below 6 pA and are therefore negligible. For the same range of voltages, we observe a change in capacitance of the device that can be understood as follows: at 0 V, the total capacitance of the device can be modeled as two capacitors in series, corresponding to the capacitance associated with the gate dielectric and capacitance corresponding to undoped multi QW stack which also behaves as a dielectric. As the voltage increases, electrons fill the QWs, and therefore, the effective thickness of the dielectric multi-QW stack decreases. For voltages above 1 V, all the QWs are filled so that the dielectric thickness now equals the constant gate dielectric thickness. Therefore, above 1 V, the capacitance saturates to the value of capacitance associated only with the gate dielectric. For negative bias applied to the metasurface, the reduction in capacitance is due to partial depletion of the highly doped $In_{0.53}Ga_{0.47}As$ layer and the QW closest to it.

To estimate the voltage-dependent optical response of the metasurface, we performed finite-difference time-domain (FDTD) simulations,[30] where we used the heterostructure described above and periodic boundary conditions to model the metasurface through a single unit cell. The permittivity for the gold layer used in the simulation was extracted from spectral ellipsometry measurements on a separate 100 nm gold film prepared under similar conditions as the devices. Since only components of the electric field which are normal to the surface can couple to the ISTs, the ISTs in the heterostructure were modeled as anisotropic harmonic oscillators following the in-plane dipole selection rules.[31] Figure 4(a) shows the simulated reflected intensity from the metasurface for two bias-voltages, 0 V and 1 V, and the inset in Fig. 4(a) shows the absolute value of the relative percent change in the reflected intensity as a function of wavelength. The simulation predicts ∼12% change in the reflectance spectrum when the electron population in the wells changes. For the same structure, our simulations predict an ∼16% decrease in the transmittance and an enhancement of absorbance by ∼45%. The absorption is enhanced because the ISTs are turned on when the bias voltage is applied.

Figure 4(b) shows experimentally measured room temperature FTIR reflectance measurements of the metasurface

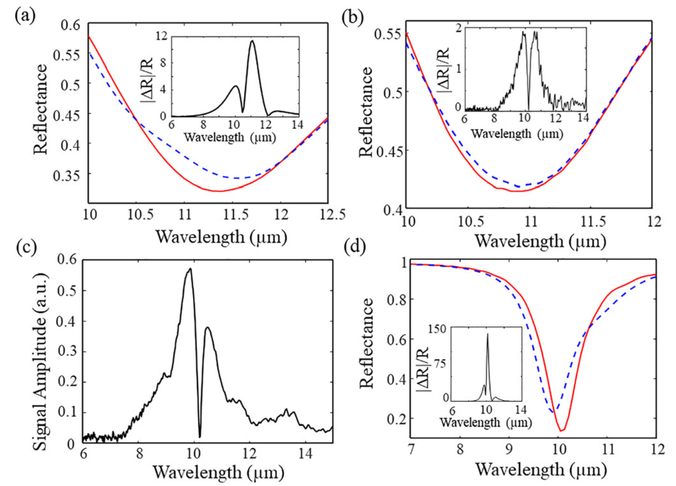

FIG. 4. (a) FDTD simulation results of reflected intensity of a metasurface with resonators of scale factor 1.35 for the two different conditions of no bias (red solid) and bias of +1 V (blue dashed). The inset shows the absolute value of the relative change in the reflected intensity in percentage, $|\Delta R|/R = |(R_{V=+1\,V} - R_{V=0})|/R_{V=0}$. (b) Room temperature FTIR reflectance measurement of a metasurface with resonators of scale factor 1.35 for the two different conditions of no bias (red solid) and bias of +1 V (blue dashed). The inset shows the absolute value of the relative change in reflectance in percentage, $|\Delta R|/R = |(R_{V=+1\,V} - R_{V=0})|/R_{V=0}$. (c) Room temperature double modulation FTIR reflectance measurement of a metasurface with resonators of scale factor 1.35. The voltage was modulated at a frequency of 10 kHz. Qualitative agreement is observed with the data shown in insets of panels (a) and (b). (d) FDTD simulation results of the reflected intensity of a metasurface with resonators of scale factor 1.35 for the two different conditions of no bias (red solid) and bias of +1 V (blue dashed) with a metal backplane. The inset shows the absolute value of the relative change in reflected intensity in percentage, $|\Delta R|/R = |(R_{V=+1\,V} - R_{V=0})|/R_{V=0}$.

for 0 V and 1 V, and the inset in Fig. 4(b) shows the absolute value of the relative percent change in the reflectance as a function of wavelength. We observe a qualitative agreement between the simulations and experiments, with an overall experimental modulation smaller than the simulated modulation. This is because the simulations assumed that the sample was illuminated by normal incidence plane waves, whereas the experiment used a microscope objective with 0.4 NA resulting in illumination with a large spread of incoming angles.[8] Since the voltage-induced change in the optical response is small, we performed a double modulation rapid-scan FTIR measurement[32] to improve the signal to noise ratio of the $\Delta R/R$ measurement. Figure 4(c) shows the change in the reflectance as a function of wavelength, measured using the double modulation. Qualitative agreement with the simulated results is again observed. To confirm that the modulated optical response of the metasurface originates from the voltage-induced change in the strength of the IST coupled to the metasurface, we repeated our double modulation FTIR measurement with metasurfaces of different scale factors. When the metasurface resonance did not spectrally overlap with the IST resonant wavelength of 11 μm, no change in the reflectance was observed. Therefore, we conclude that the modulation of the optical response was due to the voltage induced change in the strength of the ISTs coupled to the metasurface.

Finally, we discuss additional ways for enhancing the modulation of the optical response of the metasurface using this approach. This proof-of-concept design has only 4 QWs

and therefore does not provide complete spatial overlap with the optical mode. One possible way to mitigate this issue is by introducing a metal backplane underneath the highly doped $In_{0.53}Ga_{0.47}As$ layer which will significantly decrease the optical mode volume.[33] Figure 4(d) shows the simulated reflected intensity from the metasurface for 2 bias-voltages, 0 V and 1 V, but now with a metal backplane underneath the $In_{0.53}Ga_{0.47}As$ layer. The addition of metal backplane leads to reduction in the spectral width of the uncoupled metasurface resonance and induces a slight spectral shift. As shown in the inset, the simulated voltage-induced modulation, $|\Delta R|/R$, now increases by more than an order of magnitude and can be as large as 140%. Since fabrication of devices with a metal backplane requires more involved flip-chip processing, these steps will be investigated in future studies. Furthermore, future studies will also investigate other heterostructure designs that may allow a larger number of QWs and higher electron density, thereby enabling us to enhance the modulation of the optical response.[34,35]

In conclusion, we have presented a proof-of-concept experimental demonstration of a new approach for modulating the optical response of a metasurface coupled to ISTs in semiconductor QWs which uses low bias voltage and exhibits low leakage current. We demonstrated that a positive bias applied to a plasmonic metasurface resulted in enhancement of electron density in undoped quantum wells located in the near field of the metasurface. Changing the electron density in the wells modified the strength of ISTs in the wells. Since these ISTs were coupled to the metasurface resonances, changing their strength modified the reflectance of the device. Comparing experimental and simulated results, we showed that the voltage induced change in the optical response is due to coupling of the ISTs to the metasurface. Finally, we also presented directions for future studies for enhancing the modulation of the optical response of the metasurface using this approach.

This work was supported by the U.S. Department of Energy, Office of Basic Energy Sciences, Division of Materials Sciences and Engineering and performed, in part, at the Center for Integrated Nanotechnologies, an Office of Science User Facility operated for the U.S. Department of Energy (DOE) Office of Science. Sandia National Laboratories is a multi-mission laboratory managed and operated by National Technology and Engineering Solutions of Sandia, LLC, a wholly owned subsidiary of Honeywell International, Inc., for the U.S. Department of Energy's National Nuclear Security Administration under Contract No. DE-NA0003525. This paper describes objective technical results and analysis. Any subjective views or opinions that might be expressed in this paper do not necessarily represent the views of the U.S. Department of Energy or the United States Government.

[1]J. Dintinger, S. Klein, F. Bustos, W. L. Barnes, and T. W. Ebbesen, Phys. Rev. B **71**, 035424 (2005).
[2]J. Bellessa, C. Symonds, K. Vynck, A. Lemaitre, A. Brioude, L. Beaur, J. C. Plenet, P. Viste, D. Felbacq, E. Cambril, and P. Valvin, Phys. Rev. B **80**, 033303 (2009).
[3]G. Scalari, C. Maissen, D. Turcinkova, D. Hagenmuller, S. De Liberato, C. Ciuti, C. Reichl, D. Schuh, W. Wegscheider, M. Beck, and J. Faist, Science **335**(6074), 1323 (2012).
[4]D. J. Shelton, I. Brener, J. C. Ginn, M. B. Sinclair, D. W. Peters, K. R. Coffey, and G. D. Boreman, Nano Lett. **11**, 2104 (2011).
[5]Y. C. Jun, J. Reno, T. Ribaudo, E. Shaner, J. J. Greffet, S. Vassant, F. Marquier, M. Sinclair, and I. Brener, Nano Lett. **13**, 5391 (2013).
[6]J. Park, J. H. Kang, X. Liu, and M. L. Brongersma, Sci. Rep. **5**, 15754 (2015).
[7]A. Benz, S. Campione, S. Liu, I. Montano, J. F. Klem, A. Allerman, J. R. Wendt, M. B. Sinclair, F. Capolino, and I. Brener, Nat. Commun. **4**, 2882 (2013).
[8]A. Benz, I. Montano, J. F. Klem, and I. Brener, Appl. Phys. Lett. **103**, 263116 (2013).
[9]J. Lee, S. Jung, P. Y. Chen, F. Lu, F. Demmerle, G. Boehm, M. C. Amann, A. Alu, and M. A. Belkin, Adv. Opt. Mater. **2**(11), 1057 (2014).
[10]J. Lee, M. Tymchenko, C. Argyropoulos, P. Y. Chen, F. Lu, F. Demmerle, G. Boehm, M. C. Amann, A. Alu, and M. A. Belkin, Nature **511**, 65 (2014).
[11]O. Wolf, S. Campione, A. Benz, A. P. Ravikumar, S. Liu, T. S. Luk, E. A. Kadlec, E. A. Shaner, J. F. Klem, M. B. Sinclair, and I. Brener, Nat. Commun. **6**, 7667 (2015).
[12]J. Lee, N. Nookala, J. S. Gomez-Diaz, M. Tymchenko, F. Demmerle, G. Boehm, M. C. Amann, A. Alu, and M. A. Belkin, Adv. Opt. Mater. **4**(5), 664 (2016).
[13]S. Campione, A. Benz, M. B. Sinclair, F. Capolino, and I. Brener, Appl. Phys. Lett. **104**, 131104 (2014).
[14]M. Geiser, G. Scalari, F. Castellano, M. Beck, and J. Faist, Appl. Phys. Lett. **101**, 141118 (2012).
[15]Y. W. Huang, H. H. Lee, R. Sokhoyan, R. A. Pala, K. Thyagarajan, S. Han, D. P. Tsai, and H. A. Atwater, Nano Lett. **16**, 5319 (2016).
[16]J. Park, J. H. Kang, S. J. Kim, X. Liu, and M. L. Brongersma, Nano Lett. **17**, 407 (2017).
[17]A. Anopchenko, L. Tao, C. Arndt, and H. W. H. Lee, ACS Photonics **5**(7), 2631–2637 (2018).
[18]L. Ju, B. Geng, J. Horng, C. Girit, M. Martin, Z. Hao, H. A. Bechtel, X. Liang, A. Zettl, Y. R. Shen, and F. Wang, Nat. Nanotechnol. **6**, 630 (2011).
[19]N. K. Emani, T. F. Chung, A. V. Kildishev, V. M. Shalaev, Y. P. Chen, and A. Boltasseva, Nano Lett. **14**, 78 (2014).
[20]M. C. Sherrott, P. W. C. Hon, K. T. Fountaine, J. C. Garcia, S. M. Ponti, S. M. Ponti, V. W. Brar, L. A. Sweatlock, and H. A. Atwater, Nano Lett. **17**, 3027 (2017).
[21]N. Dabidian, I. Kholmanov, A. B. Khanikaev, K. Tatar, S. Trendafilov, S. H. Mousavi, C. Magnuson, R. S. Ruoff, and G. Shvets, ACS Photonics **2**, 216 (2015).
[22]Y. Yao, R. Shankar, M. A. Kats, Y. Song, J. Kong, M. Loncar, and F. Capasso, Nano Lett. **14**, 6526 (2014).
[23]R. Sarma, S. Campione, M. Goldflam, J. Shank, J. Noh, S. Smith, P. D. Ye, M. Sinclair, J. Klem, J. Wendt, I. Ruiz, S. W. Howell, and I. Brener, Appl. Phys. Lett. **113**, 061108 (2018).
[24]N. Vodjdani, B. Vinter, V. Berger, E. Bockenhoff, and E. Costard, Appl. Phys. Lett. **59**, 555 (1991).
[25]A. Majumdar, K. K. Choi, L. P. Rokhinson, J. L. Reno, and D. C. Tsui, J. Appl. Phys. **91**, 4623 (2002).
[26]K. K. Choi, B. F. Levine, C. G. Bethea, J. Walker, and R. J. Malik, Appl. Phys. Lett. **52**, 1979 (1988).
[27]A. Benz, S. Campione, J. F. Klem, M. B. Sinclair, and I. Brener, Nano Lett. **15**, 1959 (2015).
[28]A. Gabbay and I. Brener, Opt. Express **20**, 6584 (2012).
[29]R. Suzuki, N. Taoka, M. Yokoyama, S. Lee, S. H. Kim, T. Hoshii, T. Yasuda, W. Jevasuwan, T. Maeda, O. Ichikawa, N. Fukuhara, M. Hata, M. Takenaka, and S. Takagi, Appl. Phys. Lett. **100**, 132906 (2012).
[30]See https://www.lumerical.com/ for "FDTD solutions," FDTD Lumerical, Inc.
[31]S. Campione, A. Benz, J. F. Klem, M. B. Sinclair, I. Brener, and F. Capolino, Phys. Rev. B **89**, 165133 (2014).
[32]Y. G. Zhang, Y. Gu, K. Wang, X. Fang, A. Z. Li, and K. H. Liu, Rev. Sci. Instrum. **83**, 053106 (2012).
[33]A. Benz, S. Campione, S. Liu, I. Montano, J. F. Klem, M. B. Sinclair, F. Capolino, and I. Brener, Opt. Express **21**, 32572 (2013).
[34]A. Liu, Phys. Rev. B **55**, 7101 (1997).
[35]A. Gabbay, J. Reno, J. R. Wendt, A. Gin, M. C. Wanke, M. B. Sinclair, E. Shaner, and I. Brener, Appl. Phys. Lett. **98**, 203103 (2011).